Electrochemical Probes for Metal/Electrolyte System Characterization during Crevice Corrosion†

Ryan C. Wolfe,* Konrad G. Weil, and Howard W. Pickering

The Pennsylvania State University, Department of Materials Science and Engineering, 326 Steidle Building, University Park, Pennsylvania 16802

Received: January 21, 2004; In Final Form: March 10, 2004

Electrochemical microprobes for monitoring of the electrochemical conditions inside recesses are needed to better understand how localized corrosion and other charge-transfer processes occur in confined spaces. The electrode potential distribution can be routinely measured in cavities of greater than 100 μm opening dimension, but the ability to measure the concentrations of chemical species and their change with time in the presence of potential gradients is only recently becoming possible. Microprobes for potential, pH, and chloride ion will be described, and results with these sensors will be presented and discussed for creviced iron samples in aqueous electrolytes. Results reveal that these species change in concentration and distribution with time, with the greatest ionic concentrations corresponding to locations of highest metal dissolution rate on the crevice wall. These new physical chemistry insights provide a better understanding of the passive-to-active behavior in crevices.

Introduction

Crevice corrosion is a form of localized corrosion in which metal within a small space between the metal and another material corrodes at a faster rate than the outside surface of the metal. This type of corrosion is considered to be particularly insidious because it occurs in alloys that usually exhibit excellent general corrosion resistance. Another characteristic of crevice corrosion is that it takes place in areas that are not immediately visible, which can lead to unexpected catastrophic failure of the metal in service. Mitigation of crevice corrosion requires an in-depth understanding of the crevice corrosion process.

Knowledge of crevice corrosion is limited by the inability to completely characterize the crevice environment. Various techniques have been used in an attempt to quantify the crevice environment, including the extraction of crevice solution with a syringe,[1] the placement of an electrode in the path of an advancing crack, placing electrodes at fixed distances along the crevice wall,[2] capillary electrophoresis,[3] freezing and extraction of localized corrosion electrolyte,[4] and incorporation of microelectrodes in crevice formers. All these techniques are unable to obtain information at an arbitrary position within the crevice while, at the same time, observing the position of the passive to active transition on the crevice wall.

The *IR* potential drop mechanism of crevice corrosion begins with the increase in potential, φ, within the electrolyte as the anodic and cathodic reactions separate from one another.[5,6] The φ-dependent crevice corrosion behavior of a metal can be predicted from its potentiodynamic polarization curve. Figure 1 is a schematic of a metal with a crevice and the corresponding polarization curve.[7]

The metal surface at $x = 0$ is in the passive (oxide protected) region of the polarization curve, but the separation of anodic and cathodic reactions produces a potential drop, $\Delta\varphi$. This potential drop equals the decrease of the electrode potential, $E(x)$ from its value at the ($x = 0$) outer surface. Where $E(x)$ on the crevice wall is more negative than the passivation potential, E_{pass}, high rates of dissolution (i.e., crevice corrosion) will occur. In this $x > x_{pass}$ region of the crevice wall, $E(x)$ is in the active region of the polarization curve where the metal is not protected by an oxide film. E_{pass} is where the active−passive transition occurs in the polarization curve, shown on the right in Figure 1. The location of E_{pass} on the crevice wall is affected by many factors including the metal and bulk solution composition, hydrogen-ion concentration (pH), the presence of aggressive ions such as the chloride ion, and the opening dimension of the crevice, often denoted as a.

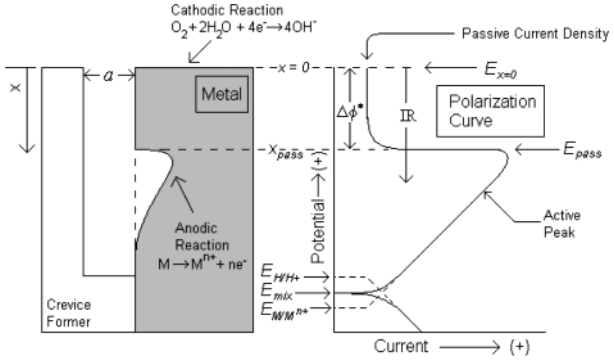

Figure 1. Schematic of a metal with a crevice (left) and its matching polarization curve (right). Metal dissolution in the crevice, denoted by the dotted line, corresponds to the active peak in the polarization curve.

The pH and aggressive ion concentration of a solution in contact with a metal has long been recognized as a major, if not primary, contributor to localized corrosion. Hydrolysis of metal cations increases the acidity of the crevice solution, and chloride anions migrate from the bulk solution into the crevice under the potential gradient $d\varphi/d\xi$ in the crevice solution. Only recently has the potential drop been documented as the main determinant of crevice corrosion in many metal/electrolyte

† Part of the special issue "Gerhard Ertl Festschrift".

* Corresponding author: phone (814) 863-7511; fax (814) 865-0122; e-mail rcw134@psu.edu.

10.1021/jp040045c CCC: $27.50
Published on Web 04/28/2004

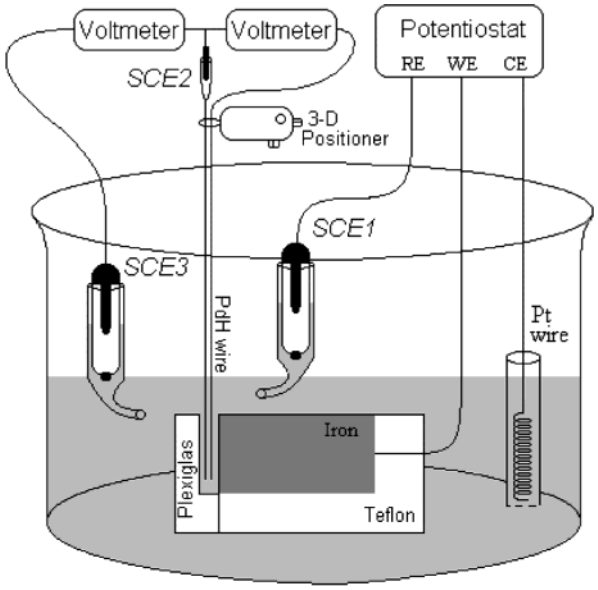

Figure 2. Schematic of the crevice corrosion cell. Microelectrodes are inserted into the crevice while the electronically isolated metal is polarized using a potentiostat.

(spontaneously active) systems. However, pH and chloride-ion changes are still important and often necessary for crevice corrosion to occur in other (spontaneously passive) systems. To understand this electrochemical behavior, it is therefore necessary to characterize the solution composition.

Researchers encounter considerable difficulty in attempting to measure the pH and concentrations of solution species (particularly chloride ions) in actual crevices because of the restricted geometry; current technology for quantifying pH in pits, crevices, and cracks is heretofore inadequate. Existing methods give rise to questions concerning accuracy due to the drastic disturbances induced during the measurement on the system being studied. No contemporary technique exists that has the flexibility of making measurements at any desired location in the crevice in real time. Therefore, electrodes capable of operation in the restricted geometries of localized corrosion sites would be of great benefit. The goal of this work is to develop a new microelectrode system that can accurately characterize the composition of the crevice electrolyte during, but without disturbing, the ongoing corrosion process. As a result of this work, the in-situ spatial concentration profiles of pH, the chloride ion, and the local electrode potential distribution were measured inside crevices.

Experimental Methods

A sensitive system recently designed and successfully implemented in this laboratory allows for the measurement of the electrode potential profile that is characteristic of, and in many cases causes, crevice corrosion. This novel microelectrode system, shown schematically in Figure 2, permits in-situ, real-time measurement of the local electrode potential inside the crevice and can be used in conjunction with small ion-specific electrodes (ISE). The metal of interest serves as the working electrode, with the counter electrode and reference electrode being comprised of a platinum wire and saturated calomel electrode (SCE), *SCE1*, respectively. The potential of the ISE sensor (which in this study is either PdH or Ag/AgCl) is measured against another SCE, *SCE2*, which has the tip of its Luggin capillary at exactly the same depth into the crevice. Both electrodes are connected to a micromanipulator and can be positioned at desired depths into the crevice. An additional SCE, *SCE3*, is used to measure the potential inside the crevice with respect to the potential in the bulk solution. Polarization curves were acquired for flat, uncreviced samples in order to understand the potential-dependent behavior inside the crevices.

The presence of a large *IR* drop poses unique challenges in the physical design of the microelectrode. The sensing length of the probe is limited not only by the desire for spatial resolution, but also by the simultaneous existence of the large *IR* voltage drop in the crevice, which can be several hundred millivolts per millimeter. A probe with a finite sensing length (which includes practically all electrodes in use) would be an inaccurate indicator of a specific ion concentration within a crevice due to the measurement of this range of *IR* voltage over the finite sensing length of the probe. The signal from such an electrode would be of the average ion concentration along this length. *IR* error can thus be avoided only by eliminating the dimension of the probe along the length of the crevice. This is accomplished by covering the wire with an insulating material and then cutting the coated wire perpendicular to its length, thereby exposing only the two-dimensional cross-sectional area of the wire electrode.

Reference Potential Microelectrode. Measurement of the local electrode potential within crevices requires a reference electrode with a Luggin capillary that is not only small enough to fit in the crevice opening, but also small enough so as to not drastically disturb the natural current distribution. For this purpose, Luggin capillaries were constructed from Pyrex glass tubing of 2 mm o.d. and a wall thickness of 0.5 mm. Using a Bunsen burner, the glass tube was heated near the two ends to form an "S" shape, with hooks facing opposite directions on the opposing ends of the tube. Hooks are formed in opposite directions in order to minimize bending of the tube during capillary formation and the subsequent straightening that must be performed. The "S"-shaped tube was secured approximately 1.5 m from the floor, and a 25 g weight was suspended from the lower hook. The middle of the straight portion of the tubing was heated for approximately 15 s using the hottest portion of the flame to heat a section approximately 3 cm long. When the strain rate reached a certain point, heating was suddenly ceased and the pull of gravity consistently formed a capillary with the outside dimension on the order of 100 μm.

Significant residual stresses are present in the glass due to the fast cooling rate and drastic elongation. These residual stresses lead to increased fragility and possible spontaneous fracture of the capillary when in service. The capillaries are particularly susceptible to breakage during the insertion of the capillary into the narrow opening of the crevice. Fractures in the drawn capillaries may also lead to electrolyte seepage, creating a short circuit in the electrochemical cell. To circumvent this problem, the capillaries were stress relieved by annealing after forming. The capillaries were annealed at 580 °C, which is 15° above the Pyrex relaxation temperature of 565 °C. Annealing for 30 min is adequate for relieving the residual stresses. The capillary was then furnace cooled. Improved toughness of the probes was obtained, and no cracks were observed in the annealed capillaries when examined by optical microscopy. These Luggin capillaries were used in the construction of the combination (pH and potential) microelectrodes.

Microelectrodes for pH Measurement. An electrode used to measure pH must consist of one electrode whose potential depends on the pH of the solution being measured and another reference electrode whose potential the former is measured against. The joined electrodes performing these two functions

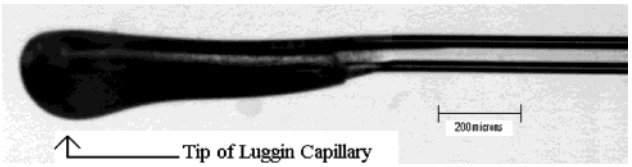

Figure 3. Optical image of a glass pH microelectrode. Only the shaded portion near the tip of the Luggin capillary is pH sensitive.

Figure 4. Optical image of a tungsten pH microelectrode.

are called a combination electrode. The unique restrictions of a crevice with a large aspect ratio require that the two electrodes be in very close proximity due to the steep potential gradients that develop at the onset of crevice corrosion.

Glass microelectrodes were produced using a modified version of the Luggin capillary preparation outlined previously. To maximize spatial resolution and minimize *IR* drop effects on the pH microelectrode, only the tip of the electrode should be sensitive to pH. To this end, the tip of the microelectrode was coated with Corning 0150 pH-sensitive glass. The pH glass was kept molten with a gas flame, while the tip of the capillary was inserted into the molten glass bead and quickly removed. Subsequent heating was required to round the features of the glass coating. An optical image of the glass pH microelectrode so produced is shown in Figure 3.

Tungsten microelectrodes have been used to study the ionic activity profile in simulated pits,[8] among other areas. A tungsten pH microelectrode, shown in Figure 4, was constructed by inserting a fine tungsten wire into the 2 mm glass tube and then drawing the tube into a fine Luggin capillary. After drawing, the capillary tip was fractured, leaving the tungsten wire intact. The tungsten wire was then extended slightly past the tip of the capillary and sealed by melting the glass. This electrode can be used in conjunction with a reference electrode to measure pH. Cracks in the glass portion of the tungsten electrode are evident in this electrode, which was made using an unannealed Luggin capillary. A second method of construction involves attaching an uninsulated tungsten wire to the side of glass capillary and then coating the entire combination with an insulating polymer. This electrode can be used for measurement of pH after surface treatment. Numerous methods of tungsten surface preparation are reported in the literature: cut,[9] polishing,[10] soaking in oxidizing solutions,[11] and flame etching.[12] The potential versus pH response of the tungsten microelectrode can be erratic due to nonuniform surface preparation techniques and the presence of dissolved oxygen.

The ability of palladium hydride to serve as a pH electrode can be understood through the palladium/hydrogen phase diagram. At room temperature, the palladium/hydrogen phase diagram consists of a low hydrogen-containing α phase, an intermediate miscibility gap consisting of two phases (α and β (also known as α') coexisting over the H/Pd atomic ratio range of 0.0089−0.609), and a high hydrogen-containing β phase. Within the α phase, the activity (or chemical potential) of hydrogen will vary depending on the amount of hydrogen in the α phase. When the hydrogen content is increased to the edge of the miscibility gap, the system is said to have only one degree of freedom (temperature), which fixes the hydrogen content and therefore the hydrogen activity of the α phase. In the two-phase region, equilibrium dictates that the activity of hydrogen in the α phase must be equal to the activity of hydrogen in the β phase. Thus, the activity of hydrogen will remain constant within this two-phase region of hydrogen content (at a constant temperature). This constant hydrogen activity in the metal provides a wide-ranging and stable hydrogen activity against which the hydrogen-ion activity in solution can be reliably measured. For a gaseous hydrogen activity of unity (analogous to a pressure of 1 atm), the pH response can be found from the Nernst equation

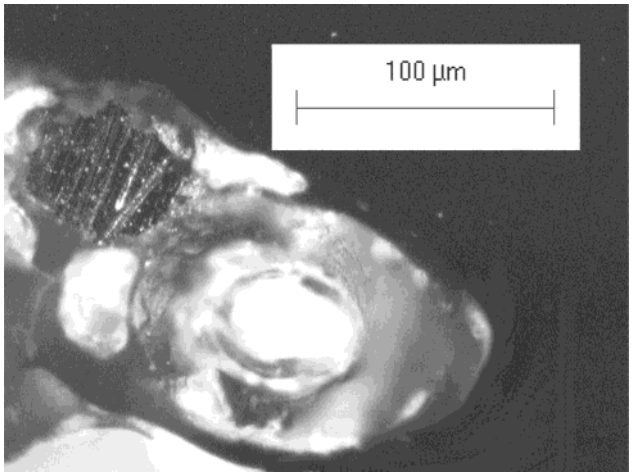

Figure 5. Cross section of the combination pH/potential microelectrode. The smaller dimension of the electrode is approximately 100 μm.

$$E = E^\circ - 2.3\frac{RT}{nF}\mathrm{pH} \qquad (1)$$

where E is the potential of the electrode, E° is the standard potential of the electrode, R is the gas constant, T is the temperature, n is the number of equivalents in the reaction, and F is the Faraday constant. This pH response is similar to the behavior of the traditional platinum/hydrogen electrode with the exception that the palladium/hydrogen electrode can be used in solutions free of gaseous hydrogen.[13] Palladium hydride provides its own source of gaseous hydrogen through absorption.

Palladium wire (99.9% purity) from Goodfellow was used to form the PdH electrode. The palladium wire, later serving as the pH-dependent electrode, was soldered to a copper wire to provide the electrical connection. The joined wire was straightened with tension and concurrent heating, and the palladium wire was attached to a Luggin capillary with an outside diameter of approximately 100 μm to serve as the reference electrode in the crevice setup. Caution must be taken to maintain the linearity of the capillary as well as to position the wire immediately next to the glass. The combination electrode was insulated with lacquer and cut to expose only the cross section of the wire to the solution, as shown in Figure 5. Additional experimental details are given elsewhere.[14]

The exposed cross section of the palladium wire was cleaned in concentrated nitric acid. A cathodic current of 10 mA cm^{-2} was applied for 60 s in Pallamerse plating solution to form palladium black on the surface. To introduce hydrogen into the palladium, deposition of hydrogen was accomplished galvanostatically by passing a cathodic current of 5 mA cm^{-2} through the electrode in deaerated solutions. All electrolyte solutions were made from reagent-grade chemicals using double-distilled water. The palladium electrode was calibrated in solutions with pH values ranging from 1 to 13 in the solutions in which hydrogen was charged. The potential of the electrode was measured using the potentiostat immediately after charging.

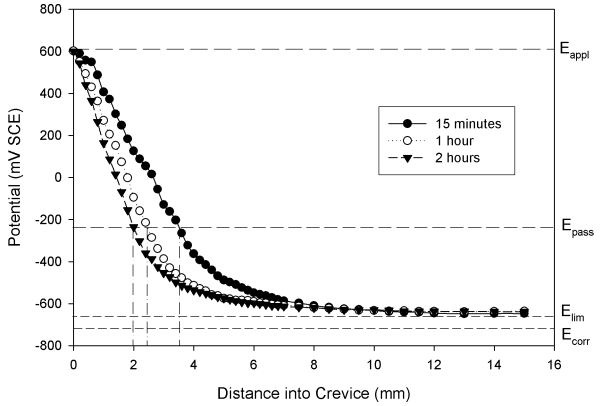

Figure 6. Potential profiles for iron in pH 6 citric acid buffer open to air with a 0.45 mm crevice opening. The passive-to-active transition, which occurred where the local potential was equal to the passivation potential, moved toward the crevice opening with time.

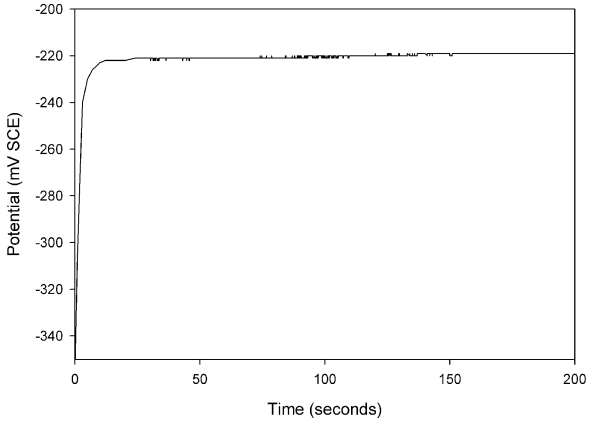

Figure 7. Potential of the palladium electrode immediately after charging in sulfuric acid solution. The response time of the PdH pH electrode is approximately 10 s.

Chloride-Ion-Specific Microelectrode. A micro-Ag/AgCl ISE is made by coating a pure silver wire (99.9985%) with lacquer to insulate the wire along its length and then cutting the wire to expose the radial cross section. The original diameter of the wire is 50 μm, while the diameter of a lacquer-coated silver wire is approximately 100 μm. After the silver wire was charged by a cathodic current of 1×10^{-7} A in 1 M NaCl solution for 30 s to get a initial uniform silver surface, it was charged by the anodic current of 3×10^{-8} A for 150 s to form AgCl. Additional details can be found elsewhere.[15]

Results and Discussion

Reference Potential Microelectrode. A crevice corrosion experiment was conducted using the setup shown in Figure 2 in 1.0 M, pH 6 citric acid buffer which is open to air with a crevice opening of $a = 0.45$ mm with the upside-down geometry. Upside-down geometry refers to a configuration in which the crevice opening faces downward, which permits convective mixing of the crevice solution with the bulk solution. This convective mixing, coupled with the use of a buffer solution, maintains a constant pH inside the crevice. The outer surface was polarized to 600 mV SCE, E_{appl}, which is in the passive region of the polarization curve. The potential profiles at 15 min, 1 h, and 2 h are shown in Figure 6. The potential drop is initially steep with a constant slope, with the slope becoming larger with increasing time. The potential starts to plateau within a few millimeters into the crevice, eventually obtaining a limiting potential, E_{lim}, which is slightly noble to the corrosion potential of uncreviced iron in the same solution, E_{corr}. It was observed that, in accordance with the theory of the *IR* mechanism of crevice corrosion, the position of the passive-to-active transition occurred on the crevice wall where the local electrode potential was equal to the passivation potential of the polarization curve. Since the pH was constant throughout the experiment, the passivation potential, E_{pass}, is shown as a constant value on the figure. At the intersection of E_{pass} with the measured potential gradient, the vertical dashed line indicates the distance into the crevice at which the passive-to-active transition was observed. The movement of the passive-to-active transition toward the opening of the crevice with time occurred simultaneously with an increase in the overall crevice corrosion current.

The potential at the bottom of the crevice, which is the most negative potential, is often referred to as the limiting potential, E_{lim}. The limiting potential was observed to be -650 mV SCE at all times, as shown in Figure 6. This is 80 mV positive of the open-circuit potential of the uncreviced metal. Possible reasons for the more positive-than-expected limiting potential include inadequate crevice depth, salt film formation, change in pH, and the presence of oxygen. Theoretically, the potential at the bottom of the crevice will never quite reach the open-circuit potential of the polarization curve. As the potential approaches the open-circuit potential, the local corrosion current decreases according to the Tafel slope. The decreasing current will produce a continually decreasing potential drop. At a potential slightly noble to the open-circuit potential, the local current will be infinitesimally small. An infinitesimally small current will produce a proportionately small potential drop. The potential in the crevice therefore will asymptotically approach the open-circuit potential of the polarization curve. Differences between the open-circuit potential of the polarization curve and the limiting potential in the crevice have been noted before and are nicely summarized in a table by Abdulsalam and Pickering.[16] The 80 mV difference between E_{corr} and E_{lim} for this system (Fe/citric acid buffer) is larger than that for the Fe/H_2SO_4 system reported in the reference, which is approximately 20 mV, but not as extreme as for the Ni/H_2SO_4 system, which is approximately 200 mV.

Palladium Hydride pH Microelectrode. The exchange current density, i_o, of the potential-determining reaction (hydrogen evolution) is an important indicator of electrode stability. Increasing i_o on the surface of an electrode is often referred to as the activation of the electrode. The degree of activation of the palladium surface can be shown by examination of the polarization curve in the Tafel region. The exchange current densities for the untreated, anodized, cyclically polarized, and palladized surfaces were 0.043, 0.638, 0.981, and 20.5 mA cm^{-2}, respectively.[7] The exchange current density for the palladized surface is large enough to resist significant depolarization by oxygen. During galvanostatic charging of the palladium with hydrogen, the potential would initially decrease for a short period of time. Measurement of the potential immediately after charging with hydrogen, Figure 7, shows the response time of the electrode. The response time is on the order of a few seconds.

The potential would then remain constant for a long period of time, on the order of hours. This pH-dependent, constant potential plateau of the two-phase region has been observed in solutions of different pH. From these data, a calibration curve can be constructed. The calibration curve so constructed is shown in Figure 8. The slope of the electrode was -58.2 mV per pH unit with an intercept of -175 mV SCE (0.067 V SHE).

At 22 °C, the slope expected based on a Nernst equation calculation is 58.5 mV pH^{-1}, which is very close to the observed

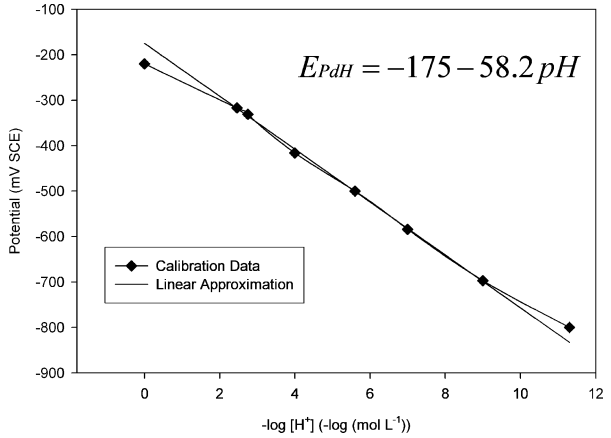

Figure 8. Calibration curve for the PdH pH electrode. Linearity in the potential response is observed from pH 2 to 9.

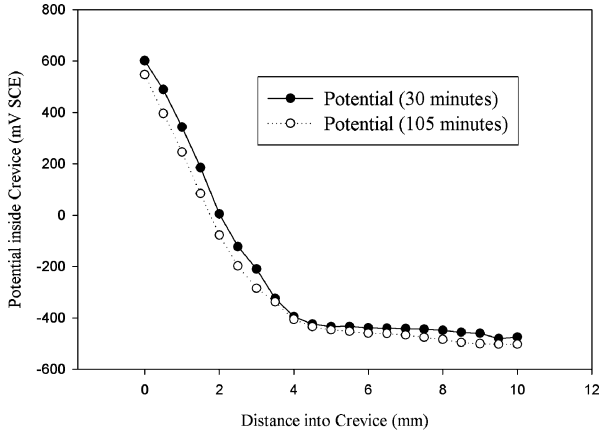

Figure 9. Potential profiles for iron in 0.5 M Na_2SO_4 ($a = 0.7$ mm). Large potential gradients are observed near the opening of crevices.

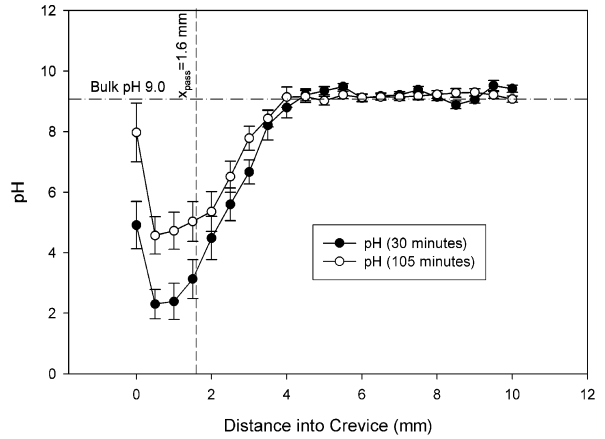

Figure 10. Profiles of pH for iron in 0.5 M Na_2SO_4 ($a = 0.7$ mm). A large decrease in pH is observed near the active region of the crevice wall.

slope of 58.2 mV pH^{-1}. The standard potential of the palladium hydride electrode naturally differs from the standard potential of the standard hydrogen electrode.[17] Even more important than adherence to theory, from a practical viewpoint, is the reproducibility of the electrode. It is the reproducibility of the electrode that will lead to the correct analysis of a solution of unknown pH upon comparison with the calibration curve. The standard deviation of the electrode potential for five experiments in 0.5 M H_2SO_4 was 6 mV or 0.1 pH. This is the experimentally determined precision of the electrode. The measured values deviate from expected behavior at the extreme acid and alkaline ends of the calibration curve. These data can be expected from the change in the activity coefficient of the hydrogen and hydroxide ions in concentrated solutions. Within the linear pH range, pH can be calculated from the best fit line, which is of the form of eq 2

$$E_{\mathrm{PdH}} = -175 - 58.2 \cdot \mathrm{pH} \qquad (2)$$

The long-term stability of the two-phase (α and β) palladium dictates the reliability of the electrode over long periods of time. The lifetime of the electrode ends when all of the β phase is lost and was determined to be at greater than 12 h. The decay mechanism is most likely due to the recombination of H atoms to form H_2 gas and the reaction of the adsorbed hydrogen with dissolved gaseous oxygen. Both of these reactions are dependent on the surface-to-volume ratio of the palladium. The greatest possible source of error for the PdH pH electrode when used in a crevice will be due to unequal positions in the crevice between the PdH electrode and the local reference electrode. If the PdH pH electrode is situated at a slightly different depth than the local reference electrode, certain corrections can be made to calculate the correct pH in the crevice.[18]

The potential and pH profiles along the length of an iron crevice in 0.5 M Na_2SO_4 are shown in Figures 9 and 10, respectively. The iron was polarized so that the potential at the opening of the crevice ($x = 0$ mm) was equal to 600 mV SCE. The potential profile exhibits an initially steep, linear region near the opening of the crevice. The potential becomes near constant near the bottom of the crevice at a potential that is slightly noble to the open-circuit potential of uncreviced iron. The pH profile, on the other hand, displays distinct minima near the opening of the crevice. The pH then maintains constant alkalinity going deeper into the crevice.

The steepness of the potential gradients (approximately 300 mV mm^{-1}) illustrates the difficulty of making accurate pH measurements in such a crevice. Despite this, however, accurate pH measurements have been made using the specialized microelectrode and cell design. The shape of the pH profile can be discussed in the context of its origin; hydrolysis by metal cations decreases the pH through the formation of a metal hydroxide. Ex-situ imaging of the crevice wall revealed that the passive-to-active transition occurred at $x = 1.6$ mm, with the majority of the dissolution occurring within a narrow band below this distance. One would then expect that the pH change within the crevice, caused by the previous dissolution of this metal, would occur at approximately this distance. Figure 10 shows precisely this behavior. The median of the pH-affected region is shifted toward the opening of the crevice, which may be due to migration caused by the strong potential field. The pH values at 30 min may be more acidic because the rate of iron dissolution (as measured by the overall crevice current, which is not shown) was greater, as compared to that at 105 min. Different pH gradients may be observed for crevices with narrower opening dimensions.

The position of the passive-to-active transition stayed relatively constant throughout the experiments at $x = 1.6$ mm. In many of these crevice experiments, particularly for narrower crevice openings, the position of the passive-to-active transition is observed to move toward the opening with time. The prevalent theory to explain this motion is that crevice corrosion results in an increase in area of the crevice wall, which leads to an increase in the overall current. The increased total crevice current creates a more precipitous drop in potential, which causes the passive-to-active transition to occur at a lower x value. An alternative explanation, based on the shifting of the pH gradient

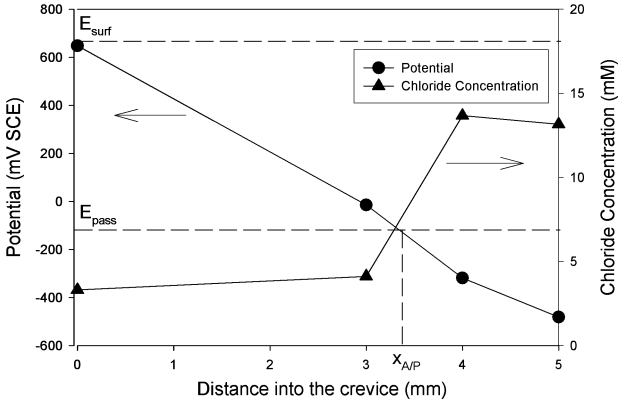

Figure 11. Local electrode potential and chloride-ion concentration profiles in the crevice with upright orientation after 10 min. The iron sample was polarized at $E_{surf} = 650$ mV (vs SCE) in 0.5M CH_3COOH + 0.5M CH_3COONa. The bulk [Cl^-] was 2 mM.[15,19]

toward the crevice opening, would be that the pH change alters the potential at which the passive-to-active transition occurs to more noble values.

Chloride-Ion-Specific Microelectrode. Calibration of the Ag/AgCl ISE showed a linear relationship in the range from 2 mM to 2 M Cl^- concentration. The slope of the calibration curve is about −58 mV/decade of [Cl^-]. The potential response can be understood from the half-cell reaction of the Ag/AgCl electrode

$$AgCl(s) + e^- \rightarrow Ag(s) + Cl^-(aq) \quad (3)$$

The electrode potential for above electrochemical reaction is given by the Nernst equation. Assuming an activity coefficient of unity for the chloride ion

$$E_{Ag/AgCl}(\text{vs SHE}) = E^\circ_{Ag/AgCl} - 0.059 \log [Cl^-] \quad (4)$$

where [Cl^-] is the Cl^- ion concentration and $E^\circ_{Ag/AgCl}$ (vs SHE) = 0.222 V at $a_{Cl-} = 1$ and 25 °C.

To investigate the role of chloride ions in the crevice corrosion of iron, anodic polarization experiments were carried out with a flat sample of pure iron in buffer solutions (pH 4.7) using 0.5 M CH_3COOH + 0.5 M CH_3COONa with chloride-ion concentrations ranging from 0 to 0.1 M.[15,19] The active−passive transition potentials, E_{pass}, were approximately −139 mV (SCE) regardless of the chloride concentration. However, as expected, the pitting potential decreased with increasing chloride-ion concentration. The passive current density increased by 1 order of magnitude with increasing chloride concentration from 0 M to 20 mM in the blank bulk solutions. When the chloride-ion concentration was 0.1 M, the passive region was not present; the pitting potential was just above E_{pass}.

For the spontaneously active system of iron in acetate-buffered solution containing chloride ions, a potential was applied to the outer surface of the crevice that was between the passivation and pitting potentials in bulk solution. The local electrode potential distribution ($E(x)$) and the in-situ chloride-ion profiles along the crevice wall were measured inside the crevice as shown in Figure 11. The transient in-situ chloride-ion profiles along the crevice wall showed that an abrupt increase in the concentration of chloride ion occurred just beyond the active/passive boundary ($x_{A/P}$) that corresponded to the active peak potential window of the anodic polarization curve.

The morphological change of the crevice wall was also observed in order to verify the accumulation of chloride ions inside the crevice during crevice corrosion. Figure 12 is an ex-situ photograph of the crevice wall showing morphological changes. The figure shows a clear passive-to-active transition at x_{pass}. Although no pitting is observed initially, pitting eventually occurred in the upper part of the passive region due to the build-up of chloride ions inside the crevice. As chloride accumulates, the pitting potential becomes more negative. Since pitting can then occur at more negative potentials, the pitting boundary, x_{pit}, moved deeper into the crevice with time.

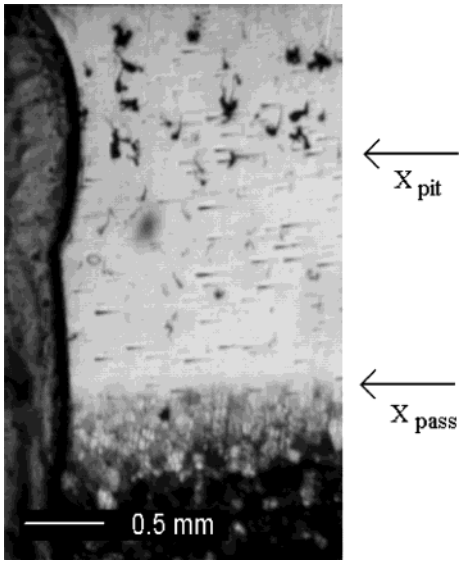

Figure 12. Ex-situ photograph of crevice wall after 25 min in 0.5M CH_3COOH + 0.5M CH_3COONa with $E_{appl} = 650$ mV(SCE). The initial [Cl^-] was 2 mM, the opening gap was 1 mm, and the length of crevice was 2 cm.[15]

Conclusions

Spatial concentration profiles of pH and the chloride ion, as well as the local electrode potential distribution, were measured inside crevices. The combination of the novel microelectrode design and experimental setup allowed these parameters to be measured at any position inside the crevice, simultaneously, while observing the position of the passive-to-active transition on the crevice wall. Data reveal that the most drastic ion concentration changes occur at this passive-to-active transition, which is the location of highest metal dissolution rate on the crevice wall. In-situ monitoring of the electrochemical conditions inside recesses using the electrochemical microprobes lends insight into how localized corrosion and other charge-transfer processes occur in confined spaces.

Acknowledgment. This work was funded by the National Science Foundation, Grant No. DMR 96-12303.

References and Notes

(1) Cho, K. H.; Abdulsalam, M. I.; Pickering, H. W. *J. Electrochem. Soc.* **1998**, *145*, 1862.

(2) Buchheit, R. G.; Moran, J. P.; Stoner, G. E. *Corrosion* **1990**, *48*, 610.

(3) Kelly, R. G.; Yuan, J.; Weyant, C. M.; Lewis, K. S. *J. Chromatogr., A* **1999**, *834*, 433.

(4) Mankowski, J.; Szklarska-Smailowska, Z. *Corros. Sci.* **1975**, *15*, 493.

(5) Pickering, H. W. *J. Electrochem. Soc.* **2003**, *150*, K1.

(6) Shaw, B. A.; McCosby, M. M.; Abdullah, A. M.; Pickering, H. W. *JOM* **2001**, *53*, 42.

(7) Pickering, H. W.; Wolfe, R. C.; Weil, K. G.; Shaw, B. A. TMS Annual Meeting & Exhibition, 2004, Charlotte, North Carolina, submitted.

(8) Luo, J. L.; Lu, Y. C.; Ives, M. B. *J. Electroanal. Chem.* **1992**, *326*, 51.
(9) Suter, T.; Böhni, H. *Electrochim. Acta* **2001**, *47*, 191.
(10) El-Basiouny, M. S.; Heakel, F.; Hefny, M. M. *Corrosion* **1981**, *37*, 175.
(11) Yao, L.; Gan, F.; Zhao, Y.; Yao, C.; Bear, J. *Corrosion* **1991**, *47*, 420.
(12) Kriksunov, L. B.; Millet, P. J.; Macdonald, D. D. *J. Electrochem. Soc.* **1994**, *141*, 3002.
(13) Vasile, M. J.; Enke, C. G. *J. Electrochem. Soc.* **1965**, *112*, 865.
(14) Wolfe, R. C. The Role of pH Development on the Localized Corrosion of Iron within the IR Mechanism of Crevice Corrosion. M.S. Thesis, The Pennsylvania State University, 2002.
(15) Won, T. Y. The Role of Chloride Ions on the Onset of Pitting within a Crevice. Ph.D. Thesis, The Pennsylvania State University, 2002.
(16) Abdulsalam, M. I.; Pickering, H. W. *Corros. Sci.* **1999**, *41*, 351.
(17) Macdonald, D. D.; Wentrcek, P. R.; Scott, A. C. *J. Electrochem. Soc.* **1980**, *127*, 1745.
(18) Wolfe, R. C.; Weil, K. G.; Pickering, H. W. *J. Electrochem. Soc.*, submitted for publication.
(19) Won, T. Y.; Pickering, H. W.; Weil, K. G. In-situ Determination of Chloride Ion Accumulation in a Corroding Model Crevice. In *203rd Meeting of the Electrochemical Society*, Paris, France, 27 April 2003; The Electrochemical Society: Pennington, NJ, 2003; Vol. 2003−01; Abstract No. 2921.